J. Biochem. 127, 681–686 (2000)

NMR Analysis of Intra- and Inter-Molecular Stems in the Dimerization Initiation Site of the HIV-1 Genome[1]

Ken-ichi Takahashi,[*] Seiki Baba,[*] Yojiro Hayashi,[*] Yoshio Koyanagi,[†] Naoki Yamamoto,[‡] Hiroshi Takaku,[*] and Gota Kawai[*,2]

[*]Department of Industrial Chemistry, Chiba Institute of Technology, 2-17-1 Tsudanuma, Narashino-shi, Chiba 275-8588; [†]Department of Virology, Tohoku University School of Medicine, 2-1 Seiryou-machi, Aoba-ku, Sendai 980-8575; and [‡]Department of Molecular Virology, Faculty of Medicine, Tokyo Medical and Dental University, 1-5-45 Yushima, Bunkyo-ku, Tokyo 113-8519

Received December 13, 1999; accepted February 3, 2000

Two positive-strand HIV-1 genomic RNAs form a dimer in virion particles through interaction of the dimerization initiation sites (DIS). The DIS RNA fragment spontaneously formed a "loose-dimer" and was converted into a "tight-dimer" by supplementation with nucleocapsid protein NCp7. This two-step dimerization reaction requires the whole DIS sequence [Takahashi *et al.* (2000) *RNA* 6, 96–102]. In the present study, we measured imino proton resonances to investigate the secondary structures of the two types of dimers in a 39-mer RNA covering the entire DIS (DIS39), including discrimination between intra- and inter-molecular base pairing. Both the presence and absence of intermolecular NOE between ^{15}N-labeled and unlabeled DIS39 were unambiguously detected in an equimolar mixture of ^{15}N-labeled and unlabeled DIS39. The stem-bulge-stem structures in both dimers were confirmed and found to be very close to each other from clear superimposition of the NMR spectra in the two dimeric states. Nevertheless, the modes of base paring in the stems of the loose- and tight-dimers were intra- and inter-molecular, respectively. Our results suggest a large structural alteration of genomic RNA occurs during virion maturation.

Key words: DIS, HIV-1, kissing-loop, NMR, RNA.

For all retroviruses, including human immunodeficiency virus type 1 (HIV-1), two molecules of genomic RNA are packaged into a virion particle in a dimeric state. This dimer formation is crucial for the maintenance of infectivity (*1–3*). *In vivo* experiments have suggested that the initial dimer changes to a more heat-stable form during protease-dependent virion maturation, including the cleavage of the gag precursor to produce nucleocapsid protein (*4*). In *in vitro* experiments, the specific sequence required for the spontaneous dimerization of HIV-1 RNA fragments was identified and named the dimerization initiation site (DIS); this site forms a stem-loop structure with a self-complementary sequence in the loop and a bulge in the stem (*5, 6*). The DIS is located close to the 5′ terminus of the genomic RNA. As a dimerization mechanism, the kissing-loop model has been proposed, in which the DIS stem-loops first dimerize by base paring between their self-complementary loop sequences (kissing-loop dimer), and then the intrastrand stems isomerize to form a stable interstrand duplex (extended-duplex dimer) (*5, 6*). The following experiments support this model since HIV-1 5′ RNA fragments containing the DIS dimerize through a two-step process: less stable dimers (loose-dimers) form spontaneously at physiological temperature after heat-denaturation, and these are then converted into more stable dimers (tight-dimers) by incubation at 55°C (*7, 8*) or at physiological temperature with the nucleocapsid protein NCp7 (*9*). It would be expected that the loose-dimers and tight-dimers correspond to the kissing-loop dimer and extended-duplex dimer, respectively. Many other experimental results also support the kissing-loop model (*1–3, 10–17*).

Recently, solution structures of two 23-mer RNAs consisting of the self-complementary loop in the DIS and its flanking stem with modified and native nucleotide sequences, respectively, have been determined by ^{1}H NMR spectroscopy. The former was reported to be in the state of the kissing-loop dimer (*18*), and the latter to be the extended-duplex dimer (*19*). In order to understand the mechanism for the conformational conversion between the two dimeric states of the DIS, however, it is necessary to use an RNA that reproduces the two-step dimerization and to compare structures of the two dimeric states of an identical oligonucleotide sequence under the same experimental conditions.

Our previous study showed that for the two-step dimerization reaction, the whole sequence of the DIS is necessary and sufficient (*20*). It has been demonstrated that part of the DIS, comprising the self-complementary loop and its

[1] This work was supported by "Research for the Future" Program (JSPS-RFTF97L00503) from the Japan Society for the Promotion of Science and, in part, by a Grant-in-Aid for High Technology Research from Ministry of Education, Science, Sports and Culture of Japan.

[2] To whom correspondence should be addressed. Phone/Fax: +81-47-478-0425, E-mail: gkawai@ic.it-chiba.ac.jp

Abbreviations: HIV-1, human immunodeficiency virus type 1; DIS, dimerization initiation site; NOE, nuclear Overhauser effect; HMQC, heteronuclear multiple quantum coherence.

flanking stem, form only the tight-dimer at physiological temperature, probably because of the low activation energy caused by the low stability of the stem. Deletion of the bulge from the DIS inhibits the NCp7-assisted conformational conversion from the loose-dimer to the tight-dimer, probably because of excess stability of the stem. On the other hand, a 39-mer RNA covering the whole DIS (DIS39) reproduces the two-step dimerization reaction: spontaneous formation of a loose-dimer and conversion into a tight-dimer in the presence of NCp7 at physiological temperatures. Adequate stability of the stem would be necessary to realize this two-step dimerization, and the presence of the bulge would be a contributing factor. Our system of DIS39 and NCp7 would be useful to investigate the molecular mechanism of the two-step dimerization of the HIV-1 genomic RNA.

In the present study, we analyzed the secondary structures of the loose- and tight-dimers in DIS39, including discrimination between intra- and inter-molecular base pairing. This discrimination will help to confirm the kissing-loop model. Since it is difficult to discriminate between intra- and inter-molecular NOE in homo-dimers by NMR spectroscopy with only ^{1}H nuclei, we used an equimolar mixture of ^{15}N-labeled and unlabeled DIS39 and succeeded in the unambiguous observation of inter-molecular NOE between labeled and unlabeled DIS39.

MATERIALS AND METHODS

Preparation of DIS39—RNA oligonucleotides of DIS39 were enzymatically synthesized by an *in vitro* transcription method with AmpliScribe T7 Transcription Kits (Epicentre Technologies, WI, USA). ^{15}N- and $^{15}N/^{13}C$-labeled RNAs were synthesized with ^{15}N- and $^{15}N/^{13}C$-labeled NTPs (Nippon Sanso, Tokyo), respectively, as substrates. All RNA samples were purified by polyacrylamide gel electrophoresis using 30 cm × 40 cm glass plates (Nihon Eido, Tokyo) under denaturing conditions with 8 M urea, and extensively desalted by ultrafiltration using Centricon YM-3 (Amicon, MA, USA). The two types of dimeric states of DIS39 were controlled in the following way. For the preparation of the loose-dimer, DIS39 in water was incubated at 95°C for 5 min and chilled on ice for 5 min. Then, the solvent was adjusted to 1× PN-buffer (10 mM sodium phosphate [pH 7.0] and 50 mM NaCl) by adding concentrated buffer. For the preparation of the tight-dimer, DIS39 in 1× PN-buffer was incubated at 95°C for 5 min and slowly cooled at room temperature. The controlled dimeric states were analyzed and confirmed by electrophoresis through non-denaturing 10% polyacrylamide gels in TBE-buffer (89 mM Tris, 89 mM borate, 2 mM EDTA) at room temperature (*20*).

NMR Measurements—DIS39 in 1× PN-buffer was concentrated to 0.3 to 0.7 mM by ultrafiltration and D_2O was added to 5%. The final volume was 200 μl. For the measurement of non-exchangeable protons, solvent H_2O was exchanged with D_2O. NMR spectra were recorded on Bruker DRX-500 and DRX-600 spectrometers at a probe temperature of 15°C. For the measurement of exchangeable protons, the solvent proton signal was suppressed by a jump-and-return pulse sequence (*21*) with delays of 65 and 50 μs for the 500 and 600 MHz spectrometers, respectively. The 1D spectra were measured by accumulating 128 to 400 scans. The ^{15}N-filtered 1D spectra of G-selectively $^{15}N/^{13}C$-labeled DIS39 were measured using the same pulse sequence for HMQC (*22*). A 3 Hz exponential multiplication and polynomial baseline correction were applied. The 2D spectra were measured using a phase sensitive mode with the States-TPPI method (*23*). 2D NOESY spectra (*24*) with a mixing time of 150 ms were recorded in 1 K × 256 complex points with 200 to 232 scans. 2D ^{13}C-^{1}H HSQC spectra (*25*) were recorded in 1 K × 64 complex points with 16 scans. Two dimensional data were processed with Gaussian window functions in both dimensions and a linear prediction in the indirect time domain to produce NOESY spectra of 2 K × 1 K real points and HSQC spectra of 2 K × 512 real points. After Fourier transformation, a polynomial baseline correction was applied.

RESULTS

NMR Signal Assignments in the Loose- and Tight-Dimers—The loose- and tight-dimers of DIS39 were prepared separately by different annealing protocols ("MATERIALS AND METHODS") and confirmed by gel electrophoresis. The two dimeric states can be distinguished by gel electrophoresis with EDTA as previously described (*20*): the loose-dimer dissociates in the gel while the tight-dimer behaves as an EDTA-resistant dimer. Figure 1 shows NOESY spectra of imino protons in the two dimeric states.

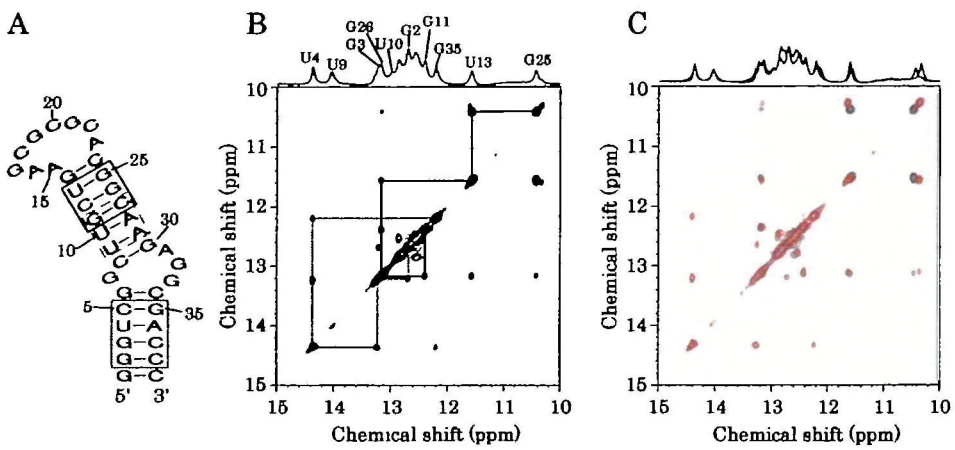

Fig. 1. **The nucleotide sequence of a predicted base pairing of DIS39 (A) and 1D and NOESY spectra of imino protons of DIS39 in the state of the loose-dimer (B and black curves in C) and tight-dimer (red curves in C) at 15°C.** NOE connectivities indicated by solid and dotted lines in B correspond to continuous base pairs as indicated by the solid and dotted boxes in A, respectively. The connectivity of base pairs indicated by broken lines in A is confirmed in Fig. 2. Assigned signals are labeled in the 1D spectrum in B.

First, for the loose-dimer, strong NOE cross-peaks between 11.57 and 10.43 ppm indicate the presence of a G:U base pair connected to two contiguous G:C base pairs according to NOE cross-peaks between the imino protons, constructing a G:U-G:C-G:C connectivity (solid lines in Fig. 1 B). This corresponds to the predicted base pair sequence, U13:G25-C12:G26-G11:C27 (solid square in Fig. 1 A). Another sequential connectivity of four base pairs, G:C-A:U-G:C-G:C, is also found (dotted lines in Fig. 1 B) corresponding to C5:G35-U4:A36-G3:C37-G2:C38 (dotted square in Fig. 1 A).

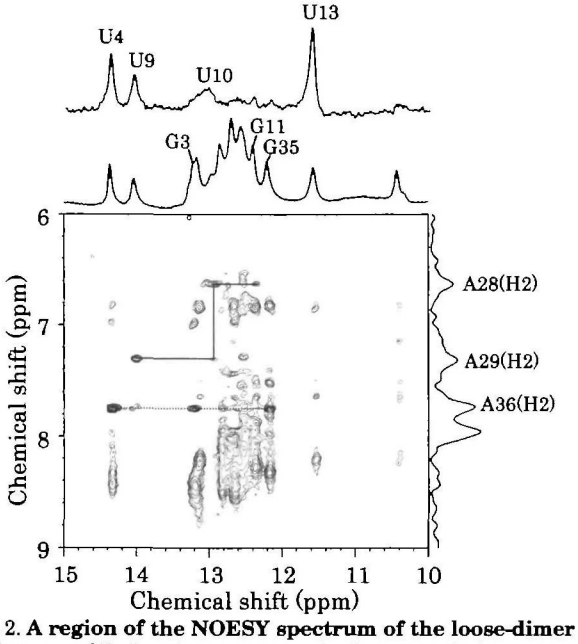

Fig. 2. **A region of the NOESY spectrum of the loose-dimer of DIS39 at 15°C showing cross-peaks between imino protons and adenosine H2 protons.** Three 1D spectra are also shown: a ^{15}N-filtered spectrum of G-selectively ^{15}N/^{13}C-labeled DIS39 in which only U imino proton resonances are observable (the top), a 1D spectrum of unlabeled DIS39 in which both G and U imino proton resonances are observable (the second top), and a 1D projection of cross-peaks between H2 protons and C2 carbons in an HSQC spectrum of A-selectively ^{15}N/^{13}C-labeled DIS39 in which only H2 proton resonances of adenosine are observable (the right-hand side). Two NOE connectivities involving H2 proton resonances are indicated (see text).

Imino proton signals of the two remaining U out of the four are clearly observed at 12.97 and 14.04 ppm in a ^{15}N-filtered 1D spectrum of G-selectively ^{15}N/^{13}C-labeled DIS39, in which only U imino proton signals are observable (the top in Fig. 2). Considering the appearance of NOE between an A H2 proton and U imino proton in an A:U base pair, and NOE between the A H2 proton and an imino proton of its neighboring base pair, a sequential connectivity of three base pairs, G:C (already assigned as G11:C27), A:U (at 12.97 ppm), and A:U (at 14.04 ppm), is found in the NOESY spectrum (solid lines in Fig. 2). This corresponds to G11:C27-U10:A28-U9:A29 (broken square in Fig. 1 A). The connectivity of C5:G35-U4:A36-G3:C37 was also confirmed using A H2 proton resonance (dotted lines in Fig. 2).

Assignments of imino proton signals in the predicted two stem regions, except the four G:C base pairs at both ends of the two stems, were achieved as described above, and summarized in Table I. There remain overlapped NOE cross-peaks between G:C base pairs at 12.86 ppm and 12.6–12.5 ppm (Fig. 1 B). These would correspond to connectivity of the 6 continuous base pairs with 2-fold symmetry, G17:C22′ through C22:G17′ in the loop-loop interaction between the two monomers in the dimeric form of DIS39 (′ represents the second monomer).

TABLE I. **Chemical shifts of imino protons of DIS39.**

	Loose-dimer (ppm)	Tight-dimer (ppm)
U13:G25	11.57	11.61
U13:**G25**	10.43	10.33
C12:**G26**	13.17	13.15
G11:C27	12.40	12.41
U10:A28	12.97	12.97
U9:A29	14.04	14.05
C5:**G35**	12.21	12.21
U4:A36	14.37	14.38
G3:C37	13.22	13.24
G2:C38	12.70	12.70

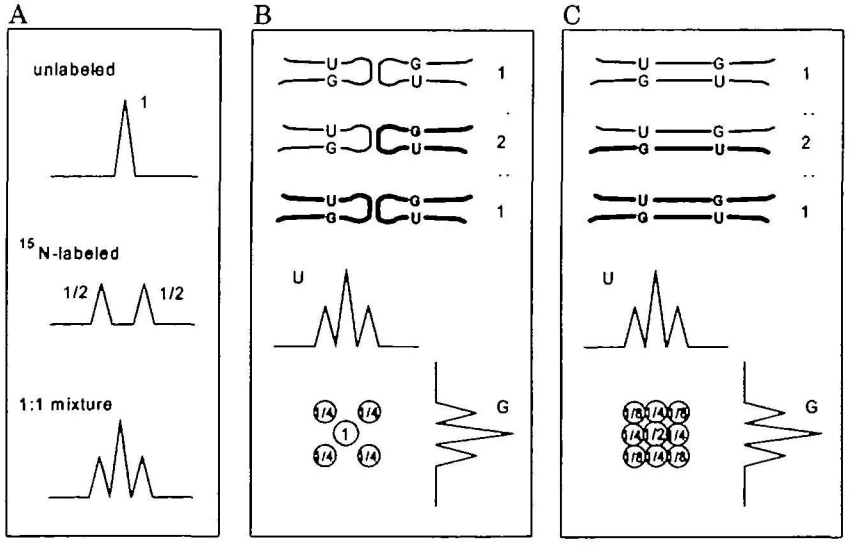

Fig. 3. **Expected patterns of 1D (A) and NOESY spectra of a 1:1 mixture of unlabeled and ^{15}N-labeled DIS39 in the states of the kissing-loop dimer (B), in which the G:U base pairs are intra-molecular, and the extended-duplex dimer (C), in which the G:U pairs are inter-molecular.** Unlabeled and ^{15}N-labeled RNAs are illustrated by thin and thick lines, respectively. The population ratio of the dimers and the signal intensity ratio are indicated. See text for details.

Signal assignments of imino protons in the tight-dimer were made in an almost identical way as for the loose-dimer because the NOESY spectra of the loose- and tight-dimers are nearly superimposable (Fig. 1 C). Differences are observed only in NOE cross-peaks involving U13, G25, G26, and base pairs in the loop region. This indicates that the structures of the two types of dimers are very close, except for the loop and its surrounding region despite the fact that the modes of base pairing in the stem are different (intra- *vs.* inter-molecular) as described below.

Discrimination of Intra- and Inter-Molecular Stems—To discriminate whether the stem is formed intra- or inter-molecularly, we investigated the presence of intermolecular NOE between U13 and G25 imino protons in an equimolar mixture of ^{15}N-labeled and unlabeled DIS39. Because ^{15}N-coupled imino proton signals are split, they can be distinguished from imino proton signals of unlabeled molecules even in a mixture (Fig. 3 A). When the mode of base pairing in the stem is intra-molecular, the U13:G25 base pair is formed either between unlabeled bases or between ^{15}N-labeled bases, but not between ^{15}N-labeled and unlabeled bases (Fig. 3 B). Thus, in this case, NOE cross-peaks should appear between unsplit signals of unlabeled bases or between split signals of ^{15}N-labeled bases, but never between split signals and unsplit signals (Fig. 3 B). In contrast, when the mode of base pairing in the stem is inter-molecular, half the population of U:G is formed between ^{15}N-labeled and unlabeled bases (Fig. 3 C). Therefore, unlike the former case, half of the total NOE volume between the U and G imino protons should appear between ^{15}N-coupled split signals and non-coupled unsplit signals (Fig. 3 C).

Figure 4 shows the region of the NOE cross-peaks between U13 and G25 imino protons in NOESY spectra of an equimolar mixture of ^{15}N-labeled and unlabeled DIS39 in the two dimeric states. In the loose-dimer state (Fig. 4 A), the pattern and intensity ratio of the NOE cross-peaks correspond closely to those in Fig. 3 B, indicating that U:G base pairing is intra-molecular in the loose-dimer. On the other hand, the pattern of the NOE cross-peaks in the tight-dimer corresponds to that in Fig. 3 C, although three vertically aligned cross-peaks fuse due to a one-fourth lower resolution in the vertical axis than in the horizontal axis (Fig. 4 B). A rough estimation shows a 1:2:1 of volume ratio for the cross-peaks between unsplit signals of unlabeled U and G, the sum of the four cross-peaks between unsplit signals and ^{15}N-coupled split signals, and the sum of the four cross-peaks between split signals. This ratio is expected when all the U:G pairs in the sample are formed inter-molecularly (Fig. 3 C). Thus, the mode of the stem in the tight-dimer appears to be inter-molecular. In conclusion, the loose- and tight-dimers of DIS39 were revealed to be the kissing-loop dimer and extended-duplex dimer, respectively. It should be noted that cross-peaks other than those between U13 and G25 could not be analyzed because of the low sensitivity.

DISCUSSION

Structural Comparison between the Kissing-Loop Dimer and Extended-Duplex Dimer—In order to reveal the molecular mechanism of the two-step dimerization reaction of the HIV-1 genomic RNA, we used a 39-mer RNA, DIS39, covering the whole DIS sequence that is necessary and sufficient to reproduce the two-step dimerization (*20*). NMR analysis of imino protons in the loose- and tight-dimers of DIS39 demonstrated the presence of a common stem-bulge-stem structure in both dimers. Furthermore, using a 1:1 mixture of ^{15}N-labeled and unlabeled DIS39, we were able to detect the presence and absence of a base pair between ^{15}N-labeled and unlabeled molecules, thus demonstrating the mode of the stem in the loose- and tight-dimers to be intra- and inter-molecular, respectively. These structural data confirm that the secondary structures of the loose- and tight-dimers correspond to the kissing-loop dimer and extended-duplex dimer, respectively, in the kissing-loop model.

Despite the difference in the mode of base pairing in the stems (intra- and inter-molecular), the superimposition of the NOESY spectra of the two types of dimers demonstrates that the structures of their stems are close to one another. On the other hand, differences in the ^{1}H chemical shifts of U13, G25, and G26 in the stem and bases in the loop demonstrate structural differences in the loop and its surrounding region between the two dimeric states. The largest difference in ^{1}H chemical shift was observed for the base pairs in the loop. A small difference was observed in

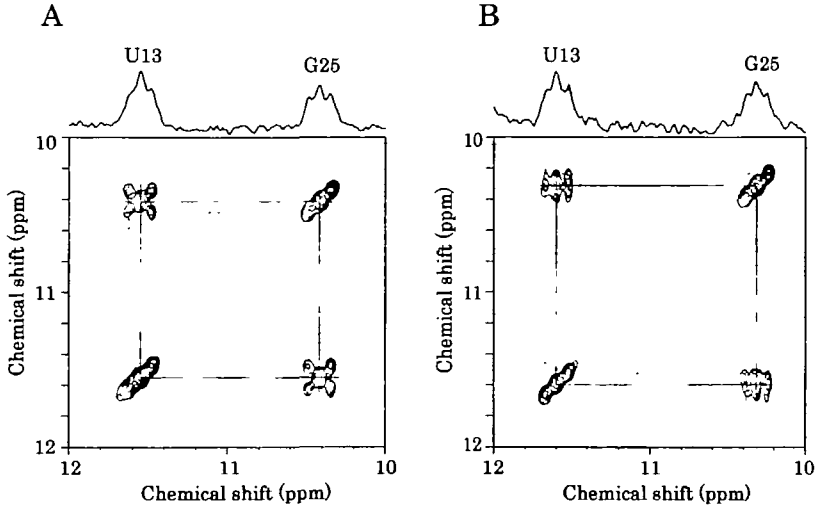

Fig. 4. **NOESY spectra of a 1:1 mixture of ^{15}N-labeled and unlabeled DIS39 in the states of the loose- (A) and tight-dimers (B) at 15°C.** A region of the U13:G25 base pair is shown. Broken and solid lines indicate proton chemical shifts for the ^{15}N-labeled and unlabeled molecules, respectively. NOE signals at the crossing of the broken and solid lines correspond exclusively to intermolecular NOE.

G25:U13 and a much smaller difference in G26:C12 in the order of distance from the loop. To investigate the structural differences between the two dimeric states in detail, NMR measurements in D_2O are in progress in our laboratory.

Solution structures of two 23-mer RNAs consisting of the self-complementary loop and its flanking stem in DIS in the state of the kissing-loop dimer (*18*) and the extended-duplex dimer (*19*), respectively, have been determined by ^1H NMR spectroscopy. The stems are in A-form for both structures. Differences between the two structures exist in the loop and nearly regions, including the extent of helical twist in the sequential six G:C base pairs in the loop, position of the three A residues in the loop, looseness of the G:C base pair closing the loop, and its way of stacking with the neighboring U:G base pair. These differences are consistent with those between the two dimeric states of DIS39 found in the present study.

Structural Characteristics of the Bulge Region—Inter-imino-proton NOE involving U9 or U10 could not be detected in both dimers of DIS39 (Fig. 1 C) their internal location within a stem. This indicates that the hydrogen bonding of the U9:A29 and U10:A28 base pairs is loosened to allow the rapid exchange of the imino protons with the solvent protons. This loosening of the stem is attributed to the presence of the 4-nt bulge because the NOE described above was clearly detected in a shortened DIS mutant without the bulge (data not shown). This is consistent with our previous observation that the bulge regulates the stability of the stem to allow conversion between the two dimeric states (*20*).

The bulge of DIS has been shown to be one of the binding sites of NC proteins (*26*). It is possible that NCp7 interacts with the bulge and loosens base paring in the stem-bulge-stem structure to the same extent in both dimers to decrease the activation energy for the conversion from the kissing-loop dimer to the extended-duplex dimer. On the other hand, we previously demonstrated that DIS25, which consists of the loop and its flanking stem with an extra G:C base pair at the end and thus does not contain the bulge, exhibited NCp7-assisted conformational conversion. Therefore, it is possible that the interaction of the stem or loop with NCp7 is more important to the annealing reaction than to the bulge. Clearly, more research is needed to understand how NCp7 works to isomerize intra-molecular stems into inter-molecular stems in DIS.

Structural Aspect of the Two-Step Dimerization in HIV-1 Virion Maturation—NMR data indicated that the structure of the stem-bulge region of DIS39 is similar in the two types of dimers. However, the 5′ and 3′ ends of one molecule of the kissing-loop dimer are close to each other whereas those of the extended-duplex dimer are located distantly from each other. Thus, the conversion of the DIS in the HIV-1 genomic RNA from the kissing-loop dimer to the extended-duplex dimer will alter the relative position between the 5′ and 3′ regions flanking the DIS, and possibly even the whole folding of the genomic RNA dimer. This structural change in the genomic RNA dimer might be related to the maturation of the virion particle.

REFERENCES

1. Laughrea, M., Jette, L., Mak, J., Kleiman, L., Liang, C., and Wainberg, M.A. (1997) Mutations in the kissing-loop hairpin of human immunodeficiency virus type 1 reduce viral infectivity as well as genomic RNA packaging and dimerization. *J. Virol.* **71**, 3397–3406
2. Clever, J.L. and Parslow, T.G. (1997) Mutant human immunodeficiency virus type 1 genomes with defects in RNA dimerization or encapsidation. *J. Virol.* **71**, 3407–3414
3. Paillart, J.C., Berthoux, L., Ottmann, M., Darlix, J.L., Marquet, R., Ehresmann, B., and Ehresmann, C. (1996) A dual role of the putative RNA dimerization initiation site of human immunodeficiency virus type 1 in genomic RNA packaging and proviral DNA synthesis. *J. Virol.* **70**, 8348–8354
4. Fu, W., Gorelick, R.J. and Rein, A. (1994) Characterization of human immunodeficiency virus type 1 dimeric RNA from wild-type and protease-defective virions. *J. Virol.* **68**, 5013–5018
5. Laughrea, M. and Jette, L. (1994) A 19-nucleotide sequence upstream of the 5′ major splice donor is part of the dimerization domain of human immunodeficiency virus 1 genomic RNA. *Biochemistry* **33**, 13464–13474
6. Skripkin, E., Paillart, J.C., Marquet, R., Ehresmann, B., and Ehresmann, C. (1994) Identification of the primary site of the human immunodeficiency virus type 1 RNA dimerization *in vitro*. *Proc. Natl. Acad. Sci. USA* **91**, 4945–4949
7. Laughrea, M. and Jette, L. (1996) Kissing-loop model of HIV-1 genome dimerization: HIV-1 RNAs can assume alternative dimeric forms, and all sequences upstream or downstream of hairpin 248–271 are dispensable for dimer formation. *Biochemistry* **35**, 1589–1598
8. Muriaux, D., Fosse, P., and Paoletti, J. (1996) A kissing complex together with a stable dimer is involved in the HIV- 1Lai RNA dimerization process *in vitro*. *Biochemistry* **35**, 5075–5082
9. Muriaux, D., De Rocquigny, H., Roques, B.P., and Paoletti, J. (1996) NCp7 activates HIV-1Lai RNA dimerization by converting a transient loop-loop complex into a stable dimer. *J. Biol. Chem.* **271**, 33686–33692
10. Laughrea, M. and Jette, L. (1996) HIV-1 genome dimerization: formation kinetics and thermal stability of dimeric HIV-1Lai RNAs are not improved by the 1–232 and 296–790 regions flanking the kissing-loop domain. *Biochemistry* **35**, 9366–9374
11. Skripkin, E., Paillart, J.C., Marquet, R., Blumenfeld, M., Ehresmann, B., and Ehresmann, C. (1996) Mechanisms of inhibition of *in vitro* dimerization of HIV type I RNA by sense and antisense oligonucleotides. *J. Biol. Chem.* **271**, 28812–28817
12. Paillart, J.C., Marquet, R., Skripkin, E., Ehresmann, B., and Ehresmann, C. (1994) Mutational analysis of the bipartite dimer linkage structure of human immunodeficiency virus type 1 genomic RNA. *J. Biol. Chem.* **269**, 27486–27493
13. Paillart, J.C., Skripkin, E., Ehresmann, B., Ehresmann, C., and Marquet, R. (1996) A loop-loop "kissing" complex is the essential part of the dimer linkage of genomic HIV-1 RNA. *Proc. Natl. Acad. Sci. USA* **93**, 5572–5577
14. Paillart, J.C., Westhof, E., Ehresmann, C., Ehresmann, B., and Marquet, R. (1997) Non-canonical interactions in a kissing loop complex: the dimerization initiation site of HIV-1 genomic RNA. *J. Mol. Biol.* **270**, 36–49
15. Muriaux, D., Girard, P.M., Bonnet-Mathoniere, B., and Paoletti, J. (1995) Dimerization of HIV-1Lai RNA at low ionic strength. An autocomplementary sequence in the 5′ leader region is evidenced by an antisense oligonucleotide. *J. Biol. Chem.* **270**, 8209–8216
16. Clever, J.L., Wong, M.L., and Parslow, T.G. (1996) Requirements for kissing-loop-mediated dimerization of human immunodeficiency virus RNA. *J. Virol.* **70**, 5902–5908
17. Haddrick, M., Lear, A.L., Cann, A.J., and Heaphy, S. (1996) Evidence that a kissing loop structure facilitates genomic RNA dimerisation in HIV-1. *J. Mol. Biol.* **259**, 58–68
18. Mujeeb, A., Clever, J.L., Billeci, T.M., James, T.L., and Parslow, T.G. (1998) Structure of the dimer initiation complex of HIV-1 genomic RNA. *Nat. Struct. Biol.* **5**, 432–436
19. Girard, F., Barbault, F., Gouyette, C., Huynh-Dinh, T., Paoletti, J., and Lancelot, G. (1999) Dimer initiation sequence of HIV-1 Lai genomic RNA: NMR solution structure of the extended

duplex. *J. Biomol. Struct. Dyn.* **16**, 1145–1157
20. Takahashi, K., Baba, S., Chattopadhyay, P., Koyanagi, Y., Yamamoto, N., Takaku, H., and Kawai, G. (2000) Structural requirement for the two-step dimerization of human immunodeficiency virus type-1 genome. *RNA* **6**, 96–102
21. Plateau, P. and Gueron, M. (1982) Exchangeable proton NMR without base-line distortion, using new strong-pulse sequence. *J. Am. Chem. Soc.* **104**, 7310–7311
22. Bax, A., Griffey, R.H., and Hawkins, B.L. (1983) Correlation of proton and nitrogen-15 chemical shifts by multiple quantum NMR. *J. Magn. Reson.* **55**, 301–315
23. Marion, D., Ikura, M., Tschudin, R., and Bax, A. (1989) Rapid recording of 2D NMR spectra without phase cycling. Application to the study of hydrogen exchange in proteins. *J. Magn. Reson.* **85**, 393–399
24. Kumar, A., Ernst, R.R., and Wuthrich, K. (1980) A two-dimensional nuclear Overhauser enhancement (2D NOE) experiment for the elucidation of complete proton-proton cross-relaxation networks in biological macromolecules. *Biochem. Biophys. Res. Commun.* **95**, 1–6
25. Bodenhausen, G. and Ruben, D.J. (1980) Natural abundance nitrogen-15 NMR by enhanced heteronuclear spectroscopy. *Chem. Phys. Lett.* **69**, 185–188
26. Damgaard, C.K., Dyhr-Mikkelsen, H., and Kjems, J. (1998) Mapping the RNA binding sites for human immunodeficiency virus type-1 Gag and NC proteins within the complete HIV-1 and -2 untranslated leader regions. *Nucleic Acids Res.* **26**, 3667–3676